Carbohydrate Polymers 97 (2013) 753–757

Contents lists available at SciVerse ScienceDirect

Carbohydrate Polymers

journal homepage: www.elsevier.com/locate/carbpol

Short communication

Mussel-inspired modification of dextran for protein-resistant coatings of titanium oxide

Jae Yoon Park[a], Jee Seon Kim[a], Yoon Sung Nam[a,b,*]

[a] Department of Material Science and Engineering, Korea Advanced Institute of Science and Technology, 291 Daehak-ro, Yuseong-gu, Daejeon 305-701, Republic of Korea

[b] KAIST Institute for NanoCentury (KINC) and BioCentury (KIB), Korea Advanced Institute of Science and Technology, 291 Daehak-ro, Yuseong-gu, Daejeon 305-701, Republic of Korea

ARTICLE INFO

Article history:
Received 4 January 2013
Received in revised form 17 May 2013
Accepted 24 May 2013
Available online 2 June 2013

Keywords:
Anti-fouling
Dextran
Catechol
Protein adsorption
Titanium dioxide

ABSTRACT

Surface modification of inorganic materials to prevent non-specific protein adsorption is critically important for developing a biocompatible materials' platform for medical implantation, diagnostics, and therapeutics. Here we report mussel-inspired chemical modification of dextran for anti-fouling coatings of metal oxide. Catechols are conjugated to dextran via a carbamate ester linkage, producing catechol-grafted dextran with a grafting density of 7.3 mol.%. Titanium dioxide (TiO_2) is coated with the catechol-grafted dextran, and the anti-fouling effect of dextran coatings is examined by using the adsorption of human serum albumin. The mussel-inspired dextran coatings show excellent resistance to non-specific protein adsorption: the adsorption equilibrium constant (K) is 0.69 L g^{-1} for dextran-coated TiO_2 while that for pristine TiO_2 surface is 3.53 L g^{-1}. This study suggests that catechol-grafted dextran is a promising material for effective anti-fouling coatings of implantable inorganic materials.

1. Introduction

There has been increasing attention on various implantable inorganic materials to preserve, restore, and replace the damaged musculoskeletal tissue. They include hydroxyapatite, aluminum, zirconium, titanium, and their oxides (Niinomi, 2008; Nomura, 2010; Ong & Chan, 2000). Titanium is one of the most commonly used materials for surgical implant due to its biocompatibility and durability in physiological environment; a thin layer (5–10 nm) of titanium is naturally oxidized into titanium dioxide (TiO_2) that eventually protects the metal body from undesirable dissolution and corrosion (MacDonald, Rapuano, & Schniepp, 2011; Raikar et al., 1995; Sul et al., 2002). Although TiO_2 is very stable compared to other materials in biological milieu, its slightly negative surface can induce blood coagulation and inflammation because of non-specific protein adsorption that can lead to the complexation of proteins with the surface metal ions, resulting in slow corrosion of titanium implant (Jackson, Omanovic, & Roscoe, 2000; Jorgenson et al., 1999; Okazaki & Gotoh, 2005; Solar, Pollack, & Korostoff, 1979).

In addition, non-specific binding of serum proteins can cause thrombosis, fibrosis, and scar tissue formation (Horbett, 1993, chap. 13; Klinger, Steinberg, Kohavi, & Sela, 1997). Therefore, protein-resistant surface modification is essentially required to maintain the biocompatibility of metallic implant materials in the body (Crotts, Sah, & Park, 1997; Jackson et al., 2000; Lee, Lee, Pyo, Park, & Lee, 2010; Lee, Park, Bae, & Park, 2013). Anti-fouling effects can be achieved by coating biomaterials with flexible and hydrophilic polymers, such as polysaccharides, phospholipids, and poly(ethylene glycol) (PEG) (Dalsin et al., 2005; Martwiset, Koh, & Chen, 2006; McArthur et al., 2000; Ye, Watanabe, Iwasaki, & Ishihara, 2003). In particular, the use of polysaccharides for anti-fouling coatings is advantageous in terms of biocompatibility and versatility for further modification. Under physiological conditions, they are found in the glycocalyx layer displayed on the surface of cellular membrane for a non-adhesive surface to effectively reduce the interaction with proteins (Holland, Qiu, Ruegsegger, & Marchant, 1998; Martwiset et al., 2006; McArthur et al., 2000; Perrino, Lee, Choi, Maruyama, & Spencer, 2008; Rich, Pearlstein, Weissmann, & Hoffstein, 1981; Sen Gupta et al., 2006). Accordingly, recent studies demonstrated that polysaccharides can be used for anti-fouling coatings of magnetic resonance imaging agents and contact lens to reduce unwanted protein adsorption and improve the biocompatibility (Tassa, Shaw, & Weissleder, 2011).

An important issue for practical applications of anti-fouling surface modification is the chemical stability of linkers used to

* Corresponding author at: Department of Material Science and Engineering, Korea Advanced Institute of Science and Technology, 291 Daehak-ro Yuseong-gu, Daejeon 305-701, Republic of Korea. Tel.: +82 42 350 3311; fax: +82 42 350 3310.
E-mail address: yoonsung@kaist.ac.kr (Y.S. Nam).

0144-8617/$ – see front matter © 2013 Elsevier Ltd. All rights reserved.
http://dx.doi.org/10.1016/j.carbpol.2013.05.064

immobilize the anti-fouling polymers to the surface of inorganic implants in physiological conditions. Surfactant-type amphiphilic polymers have been widely studied for polymer coatings. The binding of the polymers is usually mediated by hydrophobic interaction (Holland et al., 1998; Sen Gupta et al., 2006; Zhu & Marchant, 2006). Negatively charged polymers can be also used for polyelectrolyte complexation with positively charged substrates (Perrino et al., 2008). These approaches are basically based on physical interaction (hydrophobic and electrostatic interactions) of the anti-fouling polymers with the surface of inorganic implant materials, and thus the long-term stability of coatings is often questionable in physiological conditions.

Recently a mussel-inspired polymer coating has been suggested as a simple and versatile method using catechol, the side chain group of 3,4-dihydroxy-L-phenylalanine found in mussel-adhesive proteins, as a bio-mimetic adhesion molecule. Catechol and its derivatives have been employed as pendants or end groups of a pre-synthesized polymer (e.g., polyethylenimine, hyaluronic acid, polyethylene glycol, poly(vinyl alcohol), etc.) for functional coatings of various planar substrates (Kim, Lee, & Park, 2010; Lee et al., 2008). In particular, catechol is known to have a strong binding affinity to metal oxide (e.g., aluminum oxide, titanium oxide, iron oxide, etc.) through a metal–catechol coordination bond, which is robust enough to resist against thermal and hydrolytic decomposition in aqueous milieu (Kim, Kim, Kong, Park, & Nam, 2012; Lee, Lee, Messersmith, & Park, 2010; Son, Ryu, Lee, & Nam, 2013).

Here we introduce catechol-grafted dextran, denoted as 'dextran-*g*-ct', as an anti-fouling material mimicking the glycocalyx structure with a very strong binding affinity toward metal oxide. Catechols were conjugated along a chain of dextran that provides multivalent adhesion sites resulting in the stable form of immobilization. Furthermore, it is considered to have more stable adhesion than the structure of end-chain modification because this polymer structure has its functionalities on its backbone (Lee, Lee, Pyo, et al., 2010). In this study, a relatively low grafting number of catechols were conjugated to the polymer to avoid any possible interactions between unbound catechol groups and proteins (Murphy, Vollenweider, Xu, & Lee, 2010). The anti-fouling effect of dextran-*g*-ct was evaluated by measuring the adsorption isotherm of human serum albumin (HSA) on the surface of TiO_2.

2. Materials and methods

2.1. Materials

Dextran (from *Leuconostoc* spp.) with an average molecular weight of about 6 kDa, 1,1′-carbonyldiimidazole (CDI), dopamine hydrochloride, hydroquinone, and HSA were purchased from Sigma–Aldrich. Dimethylsulfoxide (DMSO), 2-propanol, and hexane were obtained from Junsei Chemical Co. P25 TiO_2 nanoparticles were obtained from Evonik-Degussa GmbH (Hanau-Wolfgang, Germany).

2.2. Synthesis and characterization of dextran-g-ct

The dextran–catechol conjugation was performed using CDI as a coupling reagent between the hydroxyl groups of dextran and the primary amine group of dopamine (Hermanson, 1996). Dextran (1.0 g, 6 mmol based on the glucose unit) was dissolved in anhydrous DMSO (7 mL). CDI (98.5 mg, 0.6 mmol) in anhydrous DMSO (3 mL) was added to the dextran solution and incubated at ambient temperature for 2 h with magnetic stirring. Dopamine hydrochloride (186.0 mg, 1.2 mmol) in anhydrous DMSO (2 mL) and hydroquinone (668.5 mg, 6 mmol) in DMSO (4 mL) were added to the CDI-activated dextran solution, followed by the further incubation at room temperature for 24 h with magnetic stirring at about 300 rpm. Dextran-*g*-ct was isolated by precipitation in a pre-chilled 6:4 mixture of 2-propanol and hexane. The precipitation process was repeated 4 times. The prepared dextran-*g*-ct was analyzed using Fourier transform infrared spectroscopy (FT-IR, JASCO) to identify the covalent bond between dextran and catechol. The ratio of catechol to the glucose unit in dextran in DMSO-d_6 was determined using ^{1}H nuclear magnetic resonance (NMR) spectroscopy (Bruker DRX 400 spectrometer) operated at 400 MHz.

2.3. TiO_2 surface modification with dextran-g-ct

P25 TiO_2 nanoparticles (100 mg) were dispersed in 25 mL of 12 mM phosphate buffered saline (PBS) at pH 7.2 by bath-type sonication. Dextran-*g*-ct (100 mg) in 12 mM PBS (25 mL) was then added to the TiO_2 dispersion and incubated at room temperature for 16 h with magnetic stirring at 300 rpm, followed by centrifugation at 3000 rpm for 30 min. The pellet was rinsed by re-dispersion with PBS. The procedures were repeated for three times.

2.4. Preparation and characterization of dextran-coated TiO_2 nanoparticles

Pristine or dextran-coated TiO_2 nanoparticles (50 mg) were dispersed in deionized water (5 mL). One drop of the TiO_2 dispersion was placed on a silicon wafer and incubated at room temperature overnight to completely remove the solvent. The dried TiO_2 sample was analyzed using transmission electron microscopy (TEM, JEOL JEM-3011 HR, Japan) at an acceleration voltage of 300 kV (Supplementary Information, Figure S1) and X-ray photoelectron spectroscopy (XPS, Sigma Probe, Thermo VG Scientific).

Supplementary material related to this article found, in the online version, at http://dx.doi.org/10.1016/j.carbpol.2013.05.064.

2.5. Protein adsorption on TiO_2 surface

Dextran-coated TiO_2 nanoparticles (100 mg) were homogeneously dispersed in PBS (25 mL). HSA was dissolved in PBS at concentrations ranging from 1.0 to 3.0 mg mL^{-1}. The dextran-coated TiO_2 dispersion and HSA solution were mixed at a volumetric ratio of 1:1 and incubated at 37 °C for pre-determined time intervals with rotary mixing at 100 rpm. The mixture was centrifuged at 14,000 rpm for 10 min. The absorbance of the supernatant was measured at a wavelength of 280 nm to determine the amount of unbound HSA.

3. Results and discussion

3.1. Characterization of the dextran-g-ct

Dopamines were conjugated to the hydroxyl groups of dextran to prepare dextran-*g*-ct (Fig. 1a). The hydroxyl groups of the glucose unit in dextran were converted to reactive carbonyl imidazole groups by using CDI as a coupling agent. Only 1:10 molar ratio of CDI to the glucose unit was used for the activation reaction because we intended to graft dopamines to relatively a small fraction of the glucose units of dextran. At high concentrations dopamines are apt to be aggregated by π–π interaction and polymerized to polydopamine via oxidation (Dreyer, Miller, Freeman, Paul, & Bielawski, 2012; Lee, Dellatore, Miller, & Messersmith, 2007), causing the resulting graft co-polymer insoluble in an aqueous solution. In particular, as the conjugation reaction proceeds, the pH of the reaction mixture increases because of the generation of imidazole. In a basic condition, dopamines are readily oxidized to initiate auto-polymerization rather than conjugated to the dextran backbone. To avoid this unwanted oxidation reaction, five-fold

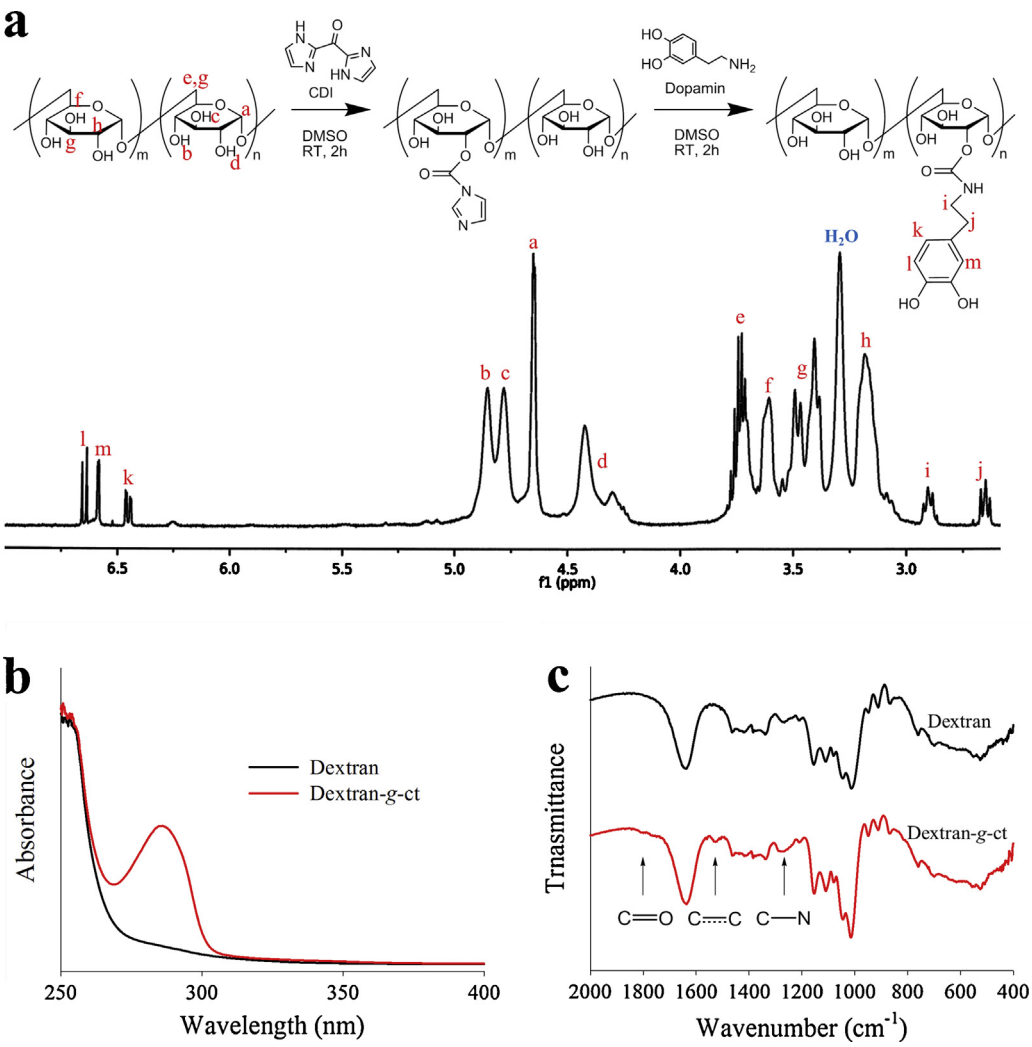

Fig. 1. (a) Schematic illustration of the synthesis procedures of dextran-*g*-ct with the ^{1}H NMR spectrum. UV–vis absorption (b) and FT-IR (c) spectra of dextran and dextran-*g*-ct.

molar excess amount of hydroquinone was added as an antioxidant to the reaction mixture. The hydroquinone was completely eliminated after the reaction as confirmed by ^{1}H NMR analysis. The generated carbonyl imidazole group is an intermediate highly susceptible to the attack by nucleophilic substances. The grafting density of catechol to dextran was determined using ^{1}H NMR analysis. The chemical shift of catechol was located at 6.4–6.6 ppm, while the characteristic peaks of dextran appeared in the range of 3.0–3.8 ppm and 4.3–5.0 ppm (Fig. 1a). In the ^{1}H NMR spectrum, the degree of substitution of catechols in dextran-*g*-ct was 7.3 mol.% as calculated from the ratio of integrated intensity of clear single hydrogen peak of glucose (*a*) and catechol (*k*). The successful grafting of catechol to dextran was also confirmed by using UV absorption spectroscopy. Dextran-*g*-ct showed a strong absorption peak around 280 nm, which is a characteristic peak for catechols, while the normal dextran had no significant absorption at the same wavelength (Fig. 1b). As calculated from the calibration curve prepared by using dopamine as a standard molecule, the molar ratio of catechol to glucose monomer units of dextran was 6 mol.%, which was roughly consistent with the ^{1}H NMR result. FT-IR analysis also confirmed that catechol was successfully conjugated to dextran by indicating the carbamate linkage between the dextran polymer and catechol (C=O stretching at 1800 cm^{-1} and C—N stretching at 1344 cm^{-1}) and the catechol group (aromatic C=C stretching at 1560 cm^{-1}) (Fig. 1c). These results indicated that catechols were successfully grafted to the dextran backbone.

3.2. Surface modification of TiO_2 with dextran-*g*-ct

The synthesized dextran-*g*-ct was used for coatings of TiO_2. It is well known that Ti atom can be readily coordinated by catechols, forming bidentate bionuclear complexes as illustrated in Fig. 2a (Anderson et al., 2010). The surface coating of TiO_2 with dextran-*g*-ct was examined through surface analysis using XPS. The presence of a nitrogen peak in the carbamate linkage, ranged from 398 to 402 eV, confirmed the successful surface coatings by dextran-*g*-ct, while the pristine TiO_2 did not show any signal in the same range of binding energy (Fig. 2b). The UV–vis absorption spectrum of dextran-coated TiO_2 was also different from that of pristine TiO_2 (Fig. 2c). This result indicates that the oxygen vacancy and oxidation states of Ti atoms seem to be affected by the interaction of TiO_2 with catechol (Iijima et al., 2008).

3.3. Anti-fouling effect of dextran coatings

The adsorption kinetics and Langmuir isotherm of HSA on pristine and dextran-coated TiO_2 were determined in 12 mM PBS (pH 7.2) at 37 °C. The nominal specific surface area of P25 TiO_2 was

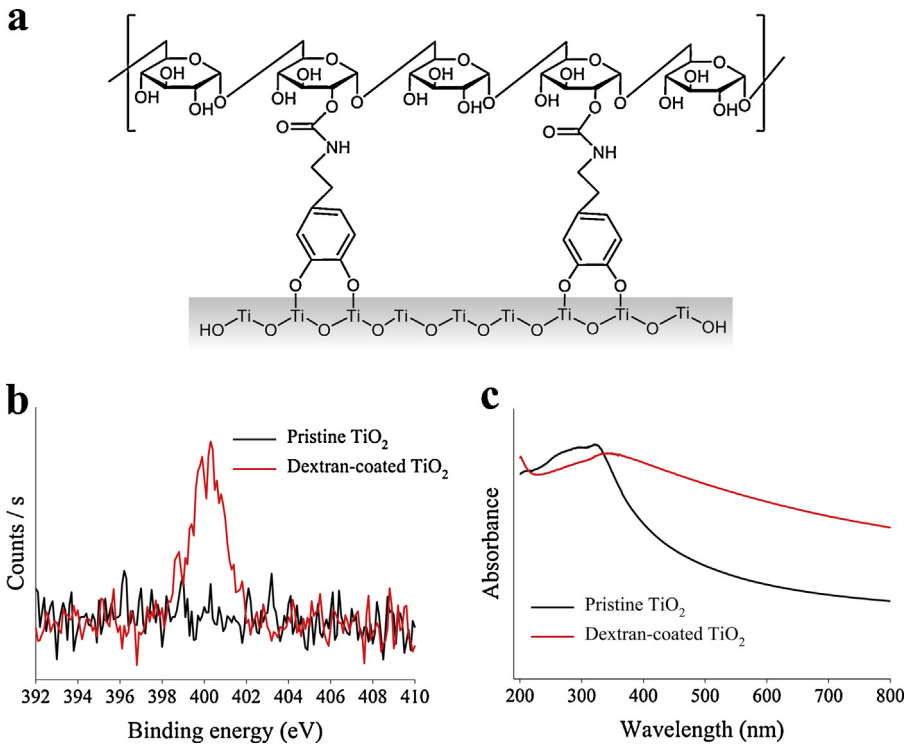

Fig. 2. (a) Schematic illustration of the catechol-mediated binding of dextran to TiO_2 surface. XP (b) and UV–vis absorption (c) spectra of pristine and dextran-coated TiO_2.

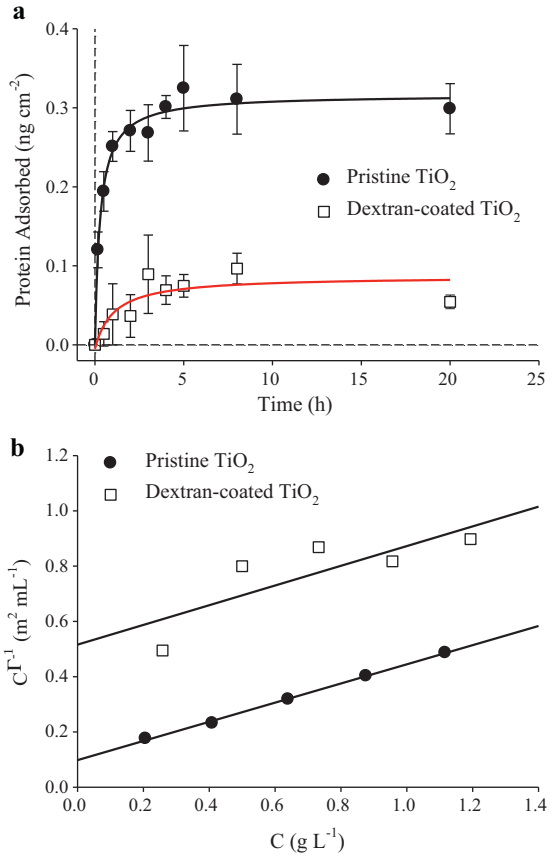

Fig. 3. Kinetic profiles (a) and linearized Langmuir isotherm (b) of HSA adsorption on pristine and dextran-coated TiO_2.

50 $m^2\ g^{-1}$. Two milligrams of TiO_2 were used in each set of experiments, and thus the total surface area of the TiO_2 samples was 0.1 m^2. For adsorption experiments, the initial concentration of HSA was fixed to 0.5 mg mL^{-1}. As the isoelectric point of HSA is about 4.7, it is negatively charged at pH 7.2. Typical saturation binding kinetics was found for HSA adsorption to the pristine and dextran-coated TiO_2 surfaces (Fig. 3a). However, the total amount of protein adsorbed on the dextran-coated surface of TiO_2 was decreased by 75%, compared to that of HSA adsorbed on pristine TiO_2, indicating excellent anti-fouling effect of dextran coating. To quantitatively determine the effect of the dextran coating on protein adsorption, the Langmuir regression curves of the adsorption isotherm of HSA on the pristine and dextran-coated TiO_2 surface were obtained (Fig. 3b). The calculated maximum amounts of HSA adsorbed per unit surface area (Γ_{max}) of pristine and dextran-coated TiO_2 were 2.88 mg m^{-2} and 2.80 mg m^{-2}, respectively. The value of Γ_{max} did not show significant change, indicating that the maximum binding site of the TiO_2 surface for HSA was almost intact; all of the binding sites will be eventually occupied in the HSA solution of an extremely high concentration. However, The calculated Langmuir equilibrium constant values (K) were 3.53 L g^{-1} and 0.69 L g^{-1} for pristine TiO_2 and dextran-coated TiO_2, respectively. The dramatic decrease of K value indicates that the dextran-coated TiO_2 surface needs much higher concentration of HSA solution than pristine TiO_2 surface to saturate the adsorption site.

4. Conclusions

Catechol-grafted dextran was synthesized and proved to be an effective coating material for anti-fouling in an aqueous milieu; about 7.3 mol.% of grafting density of catechol was detected in the modified dextran, which can form multivalent, strong binding with the TiO_2 surface in an aqueous environment at a neutral pH. Non-specific adsorption of HSA was dramatically reduced after the surface modification of TiO_2 with dextran-*g*-ct; indeed, the adsorption equilibrium constant value (K) of the dextran-coated

TiO_2 surface decreased to 0.69 L g^{-1} from 3.53 L g^{-1} for non-treated TiO_2 surface. These results suggest that the catechol-grafted dextran can be used as a promising anti-fouling coating material for titanium-based materials.

Acknowledgement

This study was supported by a grant of the Korea Healthcare Technology R&D Project, Ministry of Health & Welfare, Republic of Korea (A103017).

References

Anderson, T. H., Yu, J., Estrada, A., Hammer, M. U., Waite, J. H., & Israelachvili, J. N. (2010). The contribution of DOPA to substrate–peptide adhesion and internal cohesion of mussel-inspired synthetic peptide films. *Advanced Functional Materials*, *20*, 4196–4205.

Crotts, G., Sah, H., & Park, T. G. (1997). Adsorption determines in-vitro protein release rate from biodegradable microspheres: Quantitative analysis of surface area during degradation. *Journal of Controlled Release*, *47*, 101–111.

Dalsin, J. L., Lin, L. J., Tosatti, S., Voros, J., Textor, M., & Messersmith, P. B. (2005). Protein resistance of titanium oxide surfaces modified by biologically inspired mPEG-DOPA. *Langmuir*, *21*, 640–646.

Dreyer, D. R., Miller, D. J., Freeman, B. D., Paul, D. R., & Bielawski, C. W. (2012). Elucidating the structure of poly(dopamine). *Langmuir*, *28*, 6428–6435.

Hermanson, G. T. (1996). *Bioconjugate techniques*. San Diego: Academic Press.

Holland, N. B., Qiu, Y. X., Ruegsegger, M., & Marchant, R. E. (1998). Biomimetic engineering of non-adhesive glycocalyx-like surfaces using oligosaccharide surfactant polymers. *Nature*, *392*, 799–801.

Horbett, T. A. (1993). Principles underlying the role of adsorbed plasma proteins in blood interactions with foreign materials. *Cardiovascular Pathology*, *2*, 137–148.

Iijima, K., Goto, M., Enomoto, S., Kunugita, H., Ema, K., Tsukamoto, M., et al. (2008). Influence of oxygen vacancies on optical properties of anatase TiO_2 thin films. *Journal of Luminescence*, *128*, 911–913.

Jackson, D. R., Omanovic, S., & Roscoe, S. G. (2000). Electrochemical studies of the adsorption behavior of serum proteins on titanium. *Langmuir*, *16*, 5449–5457.

Jorgenson, D. S., Centeno, J. A., Mayer, M. H., Topper, M. J., Nossov, P. C., Mullick, F. G., et al. (1999). Biologic response to passive dissolution of titanium craniofacial microplates. *Biomaterials*, *20*(7), 675–682.

Kim, J. S., Kim, T. G., Kong, W. H., Park, T. G., & Nam, Y. S. (2012). Thermally controlled wettability of a nanoporous membrane grafted with catechol-tethered poly(N-isopropylacrylamide). *Chemical Communications*, *48*, 9227–9229.

Kim, T. G., Lee, Y., & Park, T. G. (2010). Controlled gene-eluting metal stent fabricated by bio-inspired surface modification with hyaluronic acid and deposition of DNA/PEI polyplexes. *International Journal of Pharmaceutics*, *384*, 181–188.

Klinger, A., Steinberg, D., Kohavi, D., & Sela, M. N. (1997). Mechanism of adsorption of human albumin to titanium in vitro. *Journal of Biomedical Materials Research*, *36*, 387–392.

Lee, H., Dellatore, S. M., Miller, W. M., & Messersmith, P. B. (2007). Mussel-inspired surface chemistry for multifunctional coatings. *Science*, *318*, 426–430.

Lee, H., Lee, K. D., Pyo, K. B., Park, S. Y., & Lee, H. (2010). Catechol-grafted poly(ethylene glycol) for PEGylation on versatile substrates. *Langmuir*, *26*, 3790–3793.

Lee, H., Lee, Y., Statz, A. R., Rho, J., Park, T. G., & Messersmith, P. B. (2008). Substrate-independent layer-by-layer assembly by using mussel-adhesive-inspired polymers. *Advanced Materials*, *20*, 1619–1623.

Lee, Y., Lee, H., Messersmith, P. B., & Park, T. G. (2010). A bioinspired polymeric template for 1D assembly of metallic nanoparticles, semiconductor quantum dots, and magnetic nanoparticles. *Macromolecular Rapid Communications*, *31*, 2109–2114.

Lee, Y., Park, K. M., Bae, J. W., & Park, K. D. (2013). Facile surface PEGylation via tyrosinase-catalyzed oxidative reaction for the preparation of non-fouling surfaces. *Colloids and Surfaces B: Biointerfaces*, *102*, 585–589.

MacDonald, D. E., Rapuano, B. E., & Schniepp, H. C. (2011). Surface oxide net charge of a titanium alloy: Comparison between effects of treatment with heat or radiofrequency plasma glow discharge. *Colloids and Surfaces B: Biointerfaces*, *82*, 173–181.

Martwiset, S., Koh, A. E., & Chen, W. (2006). Nonfouling characteristics of dextran-containing surfaces. *Langmuir*, *22*, 8192–8196.

McArthur, S. L., McLean, K. M., Kingshott, P., St John, H. A. W., Chatelier, R. C., & Griesser, H. J. (2000). Effect of polysaccharide structure on protein adsorption. *Colloids and Surfaces B: Biointerfaces*, *17*, 37–48.

Murphy, J. L., Vollenweider, L., Xu, F. M., & Lee, B. P. (2010). Adhesive performance of biomimetic adhesive-coated biologic scaffolds. *Biomacromolecules*, *11*, 2976–2984.

Niinomi, M. (2008). Metallic biomaterials. *Journal of Artificial Organs*, *11*, 105–110.

Nomura, N. (2010). Artificial organs: Recent progress in metals and ceramics. *Journal of Artificial Organs*, *13*, 10–12.

Okazaki, Y., & Gotoh, E. (2005). Comparison of metal release from various metallic biomaterials in vitro. *Biomaterials*, *26*, 11–21.

Ong, J. L., & Chan, D. C. N. (2000). Hydroxyapatite and their use as coatings in dental implants: A review. *Critical Reviews in Biomedical Engineering*, *28*, 667–707.

Perrino, C., Lee, S., Choi, S. W., Maruyama, A., & Spencer, N. D. (2008). A biomimetic alternative to poly(ethylene glycol) as an antifouling coating: Resistance to nonspecific protein adsorption of poly(L-lysine)-graft-dextran. *Langmuir*, *24*, 8850–8856.

Raikar, G. N., Gregory, J. C., Ong, J. L., Lucas, L. C., Lemons, J. E., Kawahara, D., et al. (1995). Surface characterization of titanium implants. *Journal of Vacuum Science & Technology A: Vacuum Surfaces and Films*, *13*, 2633–2637.

Rich, A. M., Pearlstein, E., Weissmann, G., & Hoffstein, S. T. (1981). Cartilage proteoglycans inhibit fibronectin-mediated adhesion. *Nature*, *293*, 224–226.

Sen Gupta, A., Wang, S., Link, E., Anderson, E. H., Hofmann, C., Lewandowski, J., et al. (2006). Glycocalyx-mimetic dextran-modified poly(vinyl amine) surfactant coating reduces platelet adhesion on medical-grade polycarbonate surface. *Biomaterials*, *27*, 3084–3095.

Solar, R. J., Pollack, S. R., & Korostoff, E. (1979). In vitro corrosion testing of titanium surgical implant alloys: An approach to understanding titanium release from implants. *Journal of Biomedical Materials Research*, *13*, 217–250.

Son, H. Y., Ryu, J. H., Lee, H., & Nam, Y. S. (2013). Silver-polydopamine hybrid coatings of electrospun poly(vinylalcohol) nanofibers. *Macromolecular Materials and Engineering*, *298*, 547–554.

Sul, Y. T., Johansson, C. B., Petronis, S., Krozer, A., Jeong, Y., Wennerberg, A., et al. (2002). Characteristics of the surface oxides on turned and electrochemically oxidized pure titanium implants up to dielectric breakdown: The oxide thickness, micropore configurations, surface roughness, crystal structure and chemical composition. *Biomaterials*, *23*, 491–501.

Tassa, C., Shaw, S. Y., & Weissleder, R. (2011). Dextran-coated iron oxide nanoparticles: A versatile platform for targeted molecular imaging, molecular diagnostics and therapy. *Accounts of Chemical Research*, *44*, 842–852.

Ye, S. H., Watanabe, J., Iwasaki, Y., & Ishihara, K. (2003). Antifouling blood purification membrane composed of cellulose acetate and phospholipid polymer. *Biomaterials*, *24*, 4143–4152.

Zhu, J. M., & Marchant, R. E. (2006). Dendritic saccharide surfactant polymers as antifouling interface materials to reduce platelet adhesion. *Biomacromolecules*, *7*, 1036–1041.